J. Braz. Chem. Soc., Vol. 8, No. 2, 165-168, 1997.
Printed in Brazil.

0103 – 5053 $6.00 + 0.00

Article

The Electrochemical Behavior of Brass in 0.1 M HCl Solution

E. Geler, and D.S. Azambuja*

Insituto de Química, UFRGS, Av.Bento Gonçalves 9500, C.P. 15003,

91501-970 Porto Alegre - RS, Brazil

Received: June 30, 1996; December 3, 1996

Estudou-se a eletrodissolução de um latão comercial (60,8Cu-36,3Zn-2,9Pb) e do cobre em HCl 0,1 M usando a técnica de voltametria cíclica e eletrodo rotatório de disco e anel. O mecanismo de dissolução deste latão e do cobre apresentam diferentes parâmetros cinéticos. O mecanismo de dissolução do componente Cu da liga é análogo ao do cobre puro.

The electrodissolution of commercial brass (60.8Cu-36.3Zn-2.9Pb) and pure copper in 0.1 M HCl were comparatively studied using cyclic voltammetry and a rotating ring-disk electrode. The dissolution mechanism of both specimens presents distinct kinetic parameters. However, the dissolution mechanism of the Cu component of brass is the same as that observed for pure copper.

Keywords: *copper dissolution, (α+β)-brass, rotating ring-disk electrode, voltammetry*

Introduction

The anodic dissolution of binary alloys in different aqueous environments has been investigated under a wide range of experimental conditions[1-6] mainly following a dispute between selective and simultaneous dissolution processes of the components. In this work, the dissolution of commercial brass (60.8Cu-36.3Zn-2.9Pb) in 0.1 M HCl was investigated. An understanding of the alloy dissolution mechanism requires knowledge of such a process for pure copper. Despite the number of publications on this subject[5-8], the dissolution of Cu-Zn alloys containing Pb has not received much attention. The aim of this paper is to obtain information on the electrodissolution mechanism of commercial brass in 0.1 M HCl, using cyclic voltammetry and a rotating ring-disk electrode.

Experimental Method

A conventional three electrode cell has been used. The electrochemical measurements were made using a Cu disk (99.99% pure), and one of commercial brass (60.8Cu-36.3Zn-2.9Pb) with a 0.2 cm^2 apparent area as a working electrode. Each electrode was polished with emery paper up to grade 600, and rinsed with alcohol and distilled water. To detect the formation of soluble species, during the voltammetric sweep of the working electrodes (Cu and brass) a rotating ring-disk electrode (RRDE) with a gold ring was used. The collection efficiency of the RRDE is N = 0.50[9]. For the detection of the cuprous species the ring potential was fixed at 0.45 V *vs.* SCE, in which oxidation to Cu(II) takes place. To detect the Cu(II) species, the ring potential was set at -0.1 V *vs.* SCE. A saturated calomel electrode (SCE) was used as the reference, and all potentials were referred to this electrode. A large area Pt wire, properly shielded, was used as the counter electrode. The electrolyte solutions consisted of 0.1 M HCl prepared from analytical grade reagents and twice distilled water. Experiments were carried out under Ar gas saturation at 298 K. A bipotentiostat (EG&C, model 366) and a rotator (EG&C, model 636) were employed for the measurements.

Results and Discussion

The voltammograms of Cu and brass in still 0.1 M HCl (Fig. 1), run from $E_{s,c}$ = -0.6 V to $E_{s,a}$ = 0.8 V , at 0.002 V/s, show three anodic peaks for brass, between -0.6 and -0.2 V, which are absent for Cu. At more positive potentials, two anodic peaks (A_1 and A_2) are observed and the reverse scan presents a cathodic peak (C) at more negative potentials for both working electrodes. The height of peaks A_1 and C are higher for brass. The voltammograms of Cu and brass specimens are qualitatively comparable. In the present study, the current/potential curve for brass is divided into three regions according to the prevailing process. Thus, region I

covers the potential range of -0.6 to -0.2 V, region II includes the potential range from -0.2 V up to peak A_1, and region III corresponds to the peak A_1 potential. The region of higher anodic overpotentials was not examined in this study.

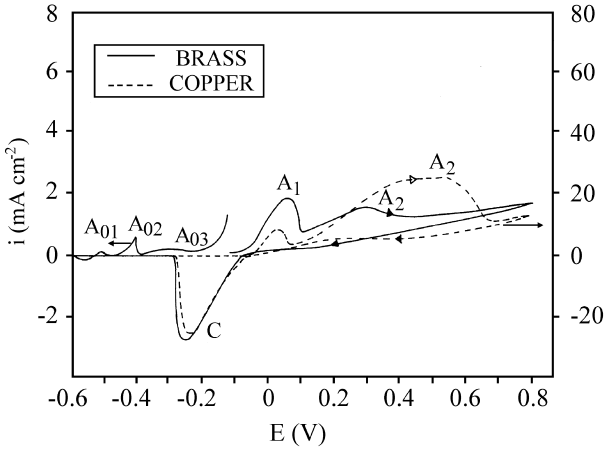

Figure 1. Voltammograms recorded at the pure Cu (.....) and brass (—) electrodes in 0.1 M HCl solution, at ν = 0.002 V/s and ω = 0.

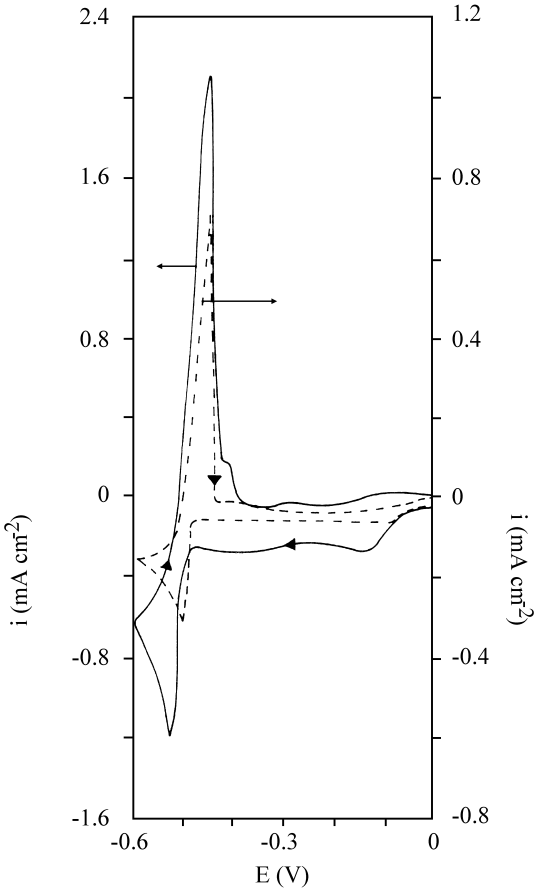

Figure 2. Voltammograms at the Au electrode in 10^{-4} M Pb^{+2} + 0.1 M HCl, at ν = 0.050 V/s (—) and ν = 0.002 V/s (—-), ω = 0.

Peak identification in region I was made by comparing the voltammograms of a Au electrode in 0.1 M HCl solution containing Pb^{+2} (Fig. 2) with the brass voltammograms (Fig. 3) in 0.1 M HCl, run from E_{sc} = -1.2 V to E_{sa} = 0 V, at ω = 0 and different scan rates. The peaks A_{01}, A_{02}, and A_{03} are associated with the presence of Pb in the alloy. This fact has been further confirmed by X-ray diffraction analysis of the brass sample[10] before and after the anodic polarization up to the A_{01} peak (not shown). As can be observed, the Pb reaction is especially significant at high sweep rates (Figs. 2 and 3), indicating a fast reaction. Selective dissolution of Zn was not observed (Fig. 3), according to thermodynamic data[2,4]. However, β phase dissolves selectively in this media, which shows up in the voltammetric curve as a shoulder, labeled as $A_β$ (Fig. 3). These results are consistent with what has been reported previously[7], which allows the characterization of the brass specimen employed in this study as a (α+β)-brass containing Pb[11]. The influence of ω on the brass voltammograms

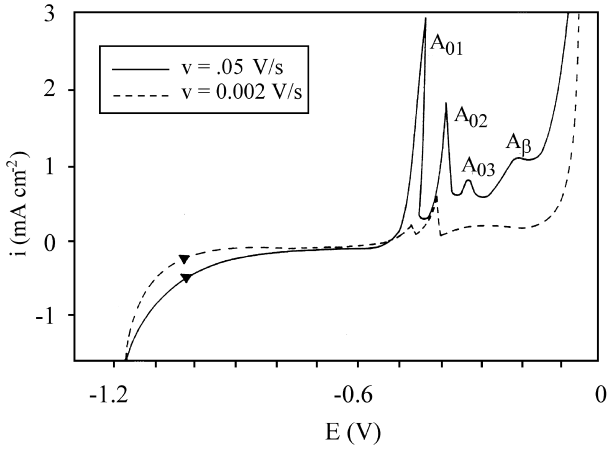

Figure 3. Voltammograms at the brass electrode in 0.1 M HCl at ν = 0.05V/s (—) and ν = 0.002V/s, ω = 0.

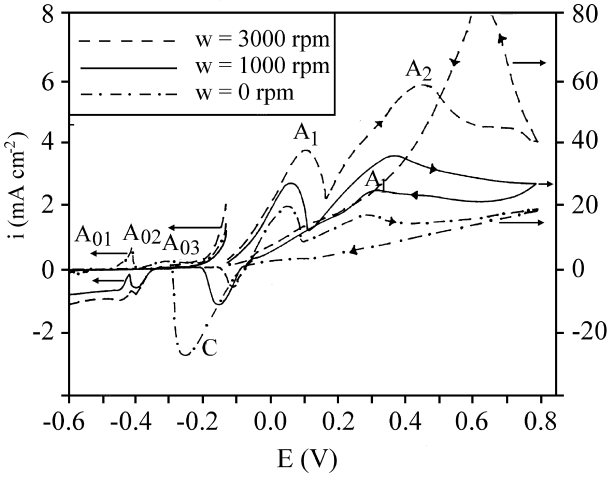

Figure 4. The influence of ω on the brass voltammograms run in 0.1 M HCl, at ν = 0.002 V/s.

at $\nu = 0.002$V/s can be seen in Fig. 4. The increase of ω results in a marked increase in height for the anodic peaks (A_1 and A_2). The reverse scan exhibits an anodic reactivation process, which increases under stirring. This behavior is similar to that obtained with pure Cu (data not shown). Apparently the rotation of the working electrodes favours the removal of part of the anodic layer, which is poorly adhered to the electrode surface. Region II is characterized by a mixed mass transfer and activation control . Plots of i^{-1} *vs.* $\omega^{-1/2}$ (Fig. 5) are straight lines with positive intercepts, and the slopes are higher for pure Cu. These results indicate that the current of the Zn component is less influenced by the mass transport effect, and are consistent with what has been previously reported for a Cu-NI alloy[12]. Furthermore, the value of the relation $(i_{E,brass} - i_{E,Cu})/ i_{E,Cu}$ was calculated for various potentials resulting in values greater than 1 in all cases. This fact suggests that the preferential dissolution of Zn also takes place in this potential range[2,4,7]. Region III corresponds to the peak A_1 potential and presents mixed control kinetics (data not shown) for both working electrodes. Table 1 shows the relation $(i_{p,brass} - i_{p,Cu}) / i_{p,Cu}$ at different sweep rates at peak A_1. The alloy components appear to dissolve at rates that are in accordance with their chemical composition. Once more, uniform dissolution takes place at this peak, and the Zn dissolution increases at a higher sweep rate.

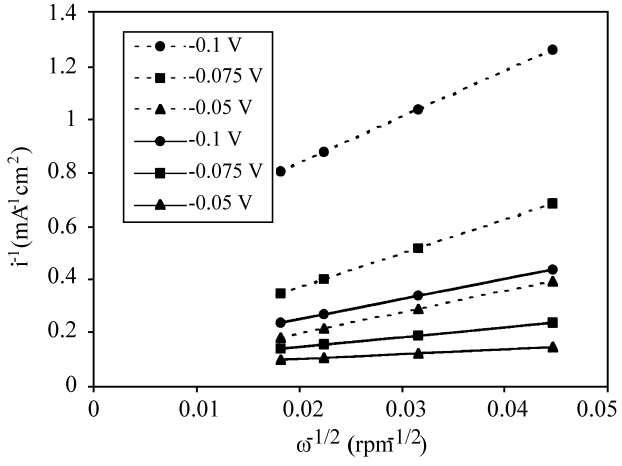

Figure 5. Plot of 1/i against $1/\omega^{1/2}$ for different potentials, for the Cu (....) and brass (—) electrodes in 0.1 M HCl.

Table 1. Dependence of the sweep rate (ν) on the relation $i_{p,brass} - i_{p,Cu} / i_{p,Cu}$ in 0.1 M HCl

Sweep rate (V/s)	$[i_{pbrass} - i_{pCu}] / i_{p,Cu}$
0.002	0.60
0.005	0.66
0.010	0.65
0.020	0.65
0.030	0.66
0.050	0.67

The rate of cuprous species formation during the dissolution of Cu and brass was monitored with the RRDE (Fig. 6b). The disk and the ring currents do not coincide in the ascending part of peak A_1 for both disks employed. For the Cu disk, this means that not all the cuprous species produced are detected by the ring, which indicates a CuCl film formation[10,13-15] which presented a maximum thickness at the potential corresponding to peak A_1. For brass, it is not possible to make similar comments since the Zn partial current was not determined. Cupric species were detected for pure copper and brass (Fig. 6c) only at higher anodic overpotentials, after exceeding the potential value of peak A_1. These findings agree with those previously reported[1,10,12-14].

The main feature of the overall process which can be derived from the RRDE data is the relation $\partial E/\partial \log i_d$, obtained in region II, and resulting in 85 mV/dec for the Cu disk and 104 mV/dec for the brass one. Calculating $\partial E/\partial i_r$,

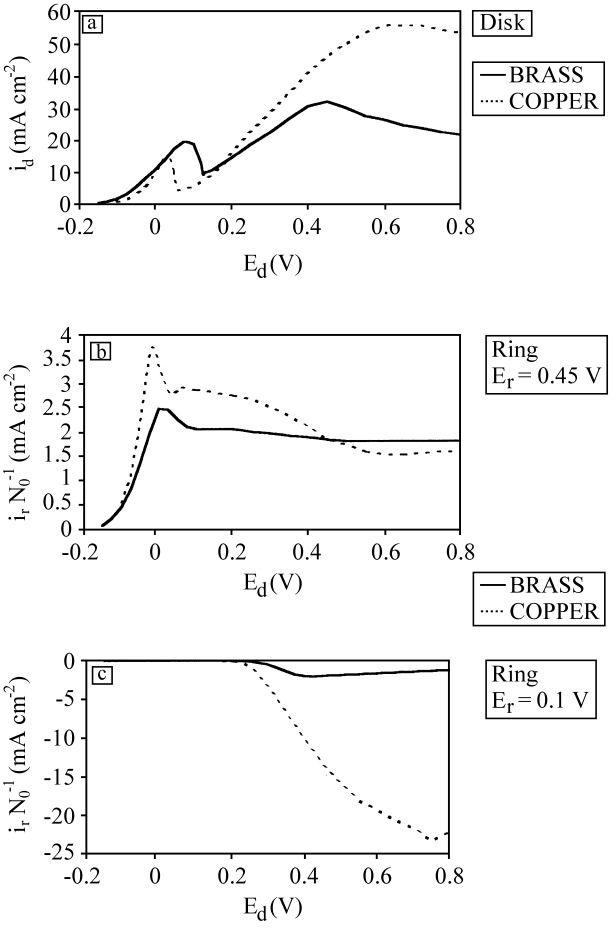

Figure 6. RRDE data. The disk current (a) and ring current at (b) $E_R = 0.45$V and $E_R = -0.1$ V (c) *vs.* disk potential run at $\nu = 0.002$ V/s and $\omega = 1000$ rpm in 0.1 M HCl.

when the ring is set at 0.45 V (the current due to the cuprous species only), a value of 96 mV/dec was found for both working disk electrodes. Again, this is a indication that although the dissolution mechanism of brass is quite different from that of copper, the dissolution mechanism of the Cu component of the alloy is the same as the one which was observed for pure copper. These results are qualitatively consistent with those reported by Costa *et al.*[13] and Lee and Nobe[14] for other Cu-Zn alloys.

Conclusions

The results of this study indicate that the electrodissolution of a **(**α+β) brass containing Pb and of pure copper in 0.1 M HCl are influenced by the mass transport effect. The dissolution mechanisms of both specimens present distinct kinetic parameters. During the electrodissolution of commercial brass, preferential dissolution of Zn occurred in the ascending part of peak A_1 and is favoured at high scan rates. The simultaneous dissolution of Cu and Zn components takes place at anodic peak A_1. The Cu component of brass behaves like pure copper during the dissolution process.

Acknowledgments

The authors wish to thank CNPq, CAPES, and FAPERGS for financial support.

References

1. Flatt, R.K.; Brook, P.A**.** *Corros. Sci.* **1971**, *11*, 185.2. Pickering,H.W.; Byrne, P.J. *J. Electrochem. Soc*. **1969**, *116* (*11*), 1492.
3. Pickering, H.W. *J. Electrochem. Soc*. **1970**, *117* (*1*), 8.
4. Taylor, A.H. *J. Electrochem. Soc*. **1971**, *118* (*6*), 854.
5 Pchelnikov, A.P.; Sitnikov, A.D.; Marshakov, I.K.; Losev, V.V. *Electrochim. Acta* **1981**, *26* (*5*), 591.
6. Polunin, A.V.; Pozdnyakova, I.A.; Pchelnikov, A.P.; Losev, V.V.; Marshakov, I.K. *Élektrokhimiya* **1982**, *18* (*6*), 792.
7. Stevanovic, J.; Skibina, L.J.; Stefanovic, M.; Despic, A.; Jovic, V.D. *J. Applied Electrochem.* **1992**, *22*, 172.
8. Vyazovikina, N.V.; Marshakov, I.K.; Tutukina, N.M. *Élektrokhimiya* **1981**, *17* (*6*), 838.
9. Albery, J.; Hitchman, M.L. In *Ring-Disc Eletrodes*; Oxford; Clarendon Press, 1971.
10. Geler, E. Master's Thesis, IQ-UFRGS 1996.
11. Suryanarayana, C.; Anantharaman, T.R. *Metallurgical Transactions* **1971**, 2, 3237.
12. Crundwell, F.K. *Electrochim. Acta* **1991**, *36* (*14*), 2135.
13. Costa, S.L.F.A. da; Agostinho, S.M.L.; Nobe, K. *J. Electrochem. Soc*. **1993**, *140* (*12*), 3483.
14. Lee, H.P.; Nobe, K.; Pearlstein, A.J. *J. Electrochem. Soc.* **1985**, *132* (*5*), 1031.
15. Crunwell, F.K. *Electrochim. Acta* **1992**, 37(*15*), 2707.